

Analysis and Design of Transmission and Drive System in Mini Surface Weapon Platform

Djoudi Farid and Li Dongguang

Abstract—This study investigates the design and analysis of the transmission and drive system in a mini-vehicle equipped with a mini-surface weapon platform. This approach can be divided into two main subjects: In the first subject a 3D-CAD model of tracked mini-vehicle that is composed of chassis and mini-surface weapon platform, which is parallel manipulators (PMs), was successfully developed to operate over a wide range of rough terrain. The designed PMs has naturally three degrees-of-freedom (3-DOF), namely: two rotations between the base and the platform (on which we focus on in this paper), and one rotation between the base and the chassis of the mini-vehicle. The second subject concerns the inverse kinematics analysis of the PMs within consideration of changes in the base orientation during the movement of the mini-vehicle on rough terrain. The goal of the PMs inverse kinematics analysis is to maintain the platform in a stable position as well as the weapon directed toward a fixed target, while the mini-vehicle is moving on rough terrain. Furthermore, a Matlab implementation of the inverse kinematics model is implemented in order to solve the PMs stabilization problem.

Index Terms—Mini-vehicle, inverse kinematics analysis, parallel manipulators (PMs), rough terrain.

I. INTRODUCTION

Combat vehicles such as tanks or infantry fighting vehicles, are the primaries striking force of land forces and they will remain so for years to come. With growing demands for improving mobility and high level of accuracy of combat vehicles over a wide range of terrain, a key feature of a military vehicle is its ability to engage target while on the move [1]. Varying operational conditions induced due to the movement of vehicle along the rough terrain pose significant challenges in maintaining the weapon directed toward the target. This led to a systematic study of vehicle terrain system, the study of overall design and kinematics of different parts composing the vehicle. The uncertainties and non flatness of the terrain also increase the complexity of both design and control task. Therefore, the main motivation of this thesis is to propose a design approach for a mini-vehicle equipped with the mini-surface weapon platform which is a PMs. Then, proceed to inverse kinematics analysis which is necessary for the PMs Stabilization control task. The designed mini-vehicle will therefore be able to handle the changes in terrain conditions.

The objective of this study is to design a tracked mini-vehicle fitted with mini-surface weapon platform which is a parallel manipulators. The designed mini-vehicle will

handle the disturbances caused by rough terrain in order to maintain the weapon platform in a stable position (horizontal plan) keeping the weapon directed toward the same fixed target.

Many studies can be found in previous works about design, stabilization and control of different numbers of degree-of-freedom (DOF) PMs. The structure of the PMs Mechanism is similar to that in Stewart platform [2].

It's clearly desirable to develop a comprehensive inverse kinematics model for effectively designing and controlling the PMs. The major objective with the inverse kinematics study is to drive explicit equations of motion for PMs. This will provide the means to understand their kinematic behavior and enable the design of more efficient devices capable of fast and accurate motions while moving on difficult terrain conditions.

In this study we will design a tracked mini-vehicle composed of two parts; chassis and mini-surface weapon platform (PMs). The tracked mini-vehicle chassis designed for exploration in rough terrain will take advantage of its design to ensure contact with the ground and overcome obstacles. The 3-DOF PMs with its base connected to the mini-vehicle chassis and a platform supporting the weapon. Then, we will proceed to inverse kinematics analysis of PMs during the movement of the mini-vehicle along rough terrain.

II. MINI VEHICLE OVERALL DESIGN

The designed mini-vehicle is a tracked type composed of two parts; chassis and mini-surface weapon platform (PMs) as shown in Fig. 1. The tracked mini-vehicle chassis designed for exploration in rough terrain takes advantage of this design to ensure contact with the ground and overcome obstacles. The 3-DOF PMs with its base connected to the mini-vehicle chassis and a platform supporting the weapon.

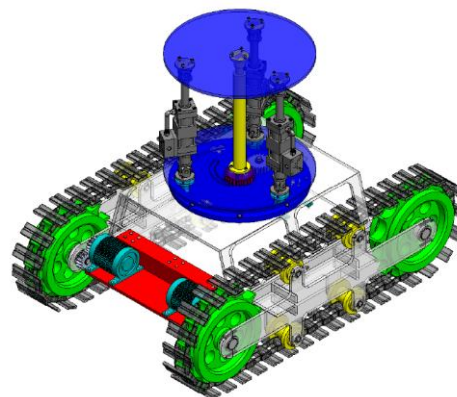


Fig. 1. Mini-vehicle overall design.

Manuscript received March 3, 2014; revised May 6, 2014.
The authors are with the School of Mechatronical Engineering, Beijing Institute of Technology, Beijing, BJ 100081 China (e-mail: gouraya.farid@yahoo.fr, Lidongguang @bit.edu.cn).

During our study, the sizing and geometry of the tracked

mini-vehicle were inspired by the Russian T90 tank. The mini vehicle design approach is adapted relatively to T90 tank geometry and dimensions so that the mini-vehicles main dimensions are calculated as one over four (1/4) of the T90 tank dimensions, with 1.7 m length, 0.9 m width and 0.45 m height. The 3D-CAD model of the mini-vehicle is built using SolidWorks.

III. MINI VEHICLE CHASSIS DESIGN

Because various manufacturers have individual design concepts and different methods of achieving the desired performance standards for the complete chassis, the choice was made to select a tracked type in order to mate the terrain conditions and carry the PMs within, whereas ensuring the platform rotation movement. It should be noted that this tracked type of chassis construction is designed to offer good downward support for the PMs and at the same time provide rotational flexibility, mainly in the region between the chassis and the PMs ensured by a gearbox cross member connected to one motor. Two other gearboxes cross member ahead of the rear suspension with two other motors to ensure the displacement of the mini-vehicle.

Due to the complexity of the variations in chassis design and because the major application of this study is the PMs movement relatively to the variation in chassis angles along the determined rough terrain, a simple chassis design is proposed in this section within all its components (Fig. 2). Therefore the mini-vehicle chassis design can be divided into two subassemblies; the chassis frame and the tracked wheel system.

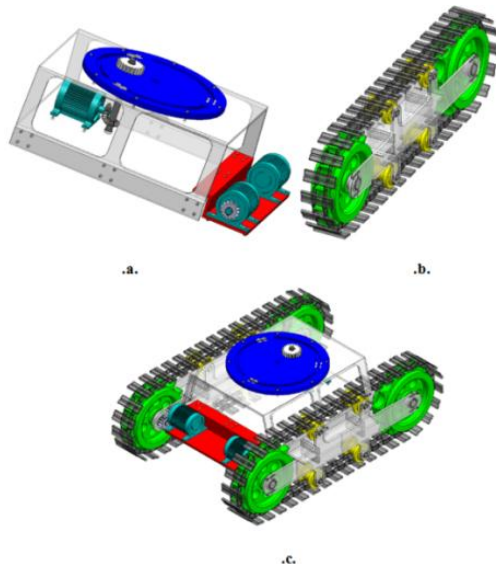


Fig. 2. a. The chassis frame b. The tracked wheel system c. The mini-vehicle chassis.

A. The Chassis Frame Model

The vehicle chassis frame is a skeleton frame on which most of the mechanical parts that include the tires, brakes, engines, and etc. are bolted. The main aim of this part is to design a chassis frame equipped with: a frame base, three motors, motor support, frame plaque and predict locations of the bolts for assembly. Two similar motors connected to spur gears providing the transmission movement to the tracked wheel system, another connected to a straight bevel gear

ensuring the yaw rotation of the PMs (Fig. 2. a).

B. The Tracked Wheel System Model

In the case of tracked vehicles like tanks, which typically operate at high speeds and often on non-flat terrain, the chain-cogwheel (tracked wheel system) design plays an important role. The modeling methodology uses a template based design which divides the chain-cogwheel mechanism into subsystems that are modeled independently. Sets of subsystems are invoked and integrated together to create a tracked wheel assembly model.

The subsystems present in the 3D-CAD model of tracked wheel mainly include: the chain, cogwheels, support rollers, cross beam, shafts, gears and bearings (Fig. 2.b). This template based design allows for easy and quick substitution of subsystems to form the final 3D-CAD model of tracked wheel. Finally, the two tracked wheel systems are assembled with the chassis frame to form a complete 3D-CAD model of the mini-vehicles chassis.

IV. 3D-CA DESIGN OF PARALLEL MANIPULATORS

Parallel manipulators are robot manipulators that consist of multiple closed-loops mechanical structure. Such manipulators gained significant interest recently due to its high accuracy, high load capacity, high rigidity, and high operation speed when compared with the conventional serial manipulators. Due to these advantages, PMs can be found in many applications, including aircraft simulators, adjustable articulated trusses, mining machines, pointing devices, and walking machines. One of the first applications of this type of mechanisms is believed to be the tire testing machine introduced by Gough and White wall [3], followed by the motion simulation platform built by Stewart [2]. Recent research works also involve design and analysis for less degree-of-freedom devices having 3, 4, and 5-DOF. One early example is a novel translational 3-DOF parallel mechanism employing UPU chain structure [4], [5].

TABLE I: NOMENCLATURE OF 3D-CAD MODEL OF THE PARALLEL MANIPULATORS

N ^o	Designation	Number	Characteristics
1	Socket head cap Screw	21	ISO 4762 - M8 x 30
2	Cylindrical Joint	6	
3	Hexagon Nut	24	ISO - 4034 - M8 - S
4	Washer	48	ISO 7089 - 8
5	Hexagon Bolt	24	
6	Plus Link	6	
7	Ball Joint	1	
8	Ball	1	
9	Central Leg	1	
10	Active actuator	3	HMX series of Parker's EH cylinders
11	Socket head cap Screw	3	ISO 4762 - M8 x 35
12	Prismatic Joint	3	
13	Spur Gear	1	ISO-Spur gear 5M-27T-20PA-30FW
14	Circlip	1	Circlip DIN 471 - 30 x 3,5
15	Base	1	
16	Platform	1	

The stabilized PMs in Fig. 3 consists of three main parts, namely: the base (15) which is not controlled in any way by

actuators, moving platform (16), which is connected to the base by three active actuators (10) and one central leg (9).

Table I illustrates nomenclature of different parts composing the PMs Structure implicitly shown in Fig. 3.

A. The Base Structure

Gears mechanism composed of two spur gears was forecasted between the base (15) and the frame plaque which allows a 60° (30° left and 30° right) yaw rotation of the PMs

relatively to the mini-vehicle chassis. Three circular prismatic grooves of 110° have been performed on the frame plaque allowing the sliding movement of the three prismatic joints (12) during the yaw rotation of the PMs. Another circular prismatic groove of 60° has been performed on the base which allows the sliding movement of the shaft connected to one motor during the yaw rotation of the PMs. The central leg is fixed in the middle of the base (Fig. 3).

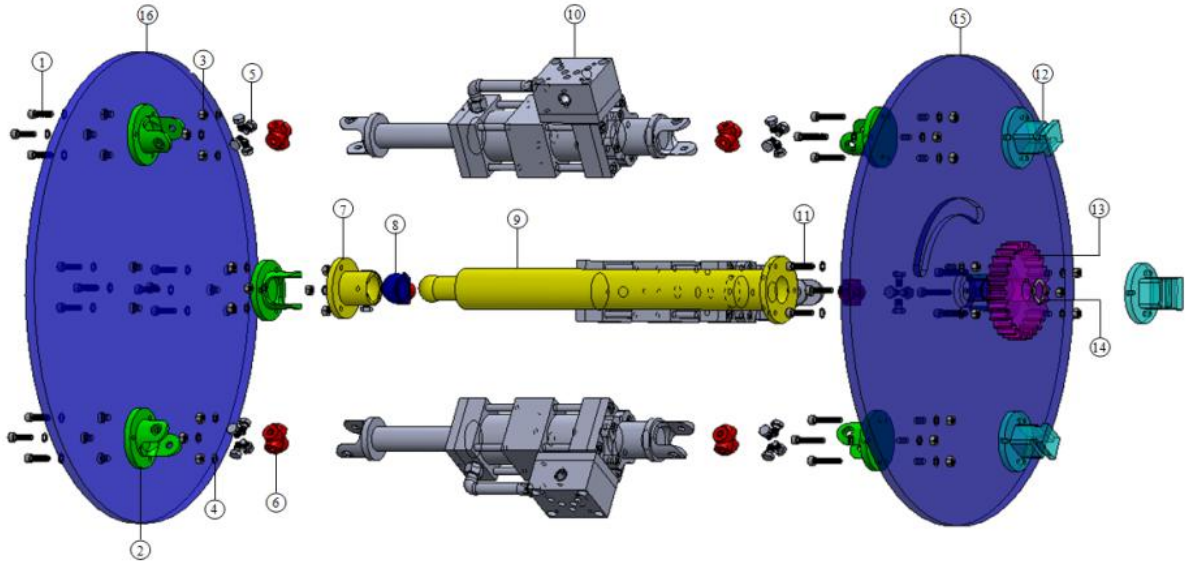


Fig. 3. 3D-CAD Model of the parallel manipulators mechanisms.

B. The Parallel Manipulators Actuator

Nowadays, actuating robotic systems is still one of the biggest challenges. High performances in actuation are needed to enhance behaviors of these systems, whereas more and more requirements are needed for best performance [6].

The design of the actuators allows moving whose result is its extension and shortening which enable the pitch and roll rotation movements of the PMs Platform. The actuator design proposed in this part is based on HMIX series of Parker's electro-hydraulic cylinders, with necessary changes to fit the designed PMs (Fig. 4). The designed cylinder has a stroke of 165 mm which can enable approximately 60 degrees pitch and roll rotation movements of the PMs Platform.

For better adaptation and control of the PMs, the designed actuator includes an internally mounted magnetostrictive transducer to provide continuous analog or digital feedback of the actuator's position.

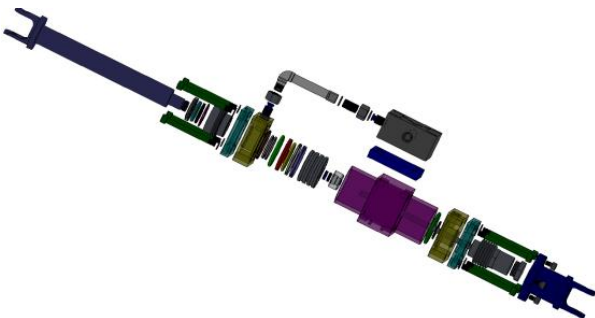


Fig. 4. Exploded view of the 3D-CAD actuator model.

C. The Platform Structure

The platform is the upper part of the PMs supporting the

weapon system. It is connected to three actuators by cylindrical joints and connected to the central leg by a spherical joint (Fig. 3). This designed platform can perform two rotational movements pitch and roll of 60 degrees (30° degrees up and 30° degrees down).

V. TOLERANCE ANALYSIS OF THE PARALLEL MANIPULATORS

The analysis of causes and effects of dimensional and geometric variations is a major concern in the design and manufacture of mechanical products.

The purpose of tolerance analysis is to study the accumulation of variations on a geometric attribute of interest (dimension, location, orientation etc.). To incorporate a design improvement study and note the effects on the global shape and geometry of the PMs, mechanical design solutions and tolerances study will be investigated. The tolerance analysis of the PMs was done for each part of the 3D-CAD model composing the PMs as shown in Fig. 5.

VI. INVERSE KINEMATICS ANALYSIS OF THE PARALLEL MANIPULATORS

Kinematics analysis is the basis for PMs Design and control, and study of kinematics is a subject that deserves in-depth exploration [7]. Kinematics and practical design consideration have been discussed in several publications [8], [9].

A. Description and Mobility Analysis

The PMs studied in this work is a 3-DOF mechanism

where, 1-DOF (yaw rotation) is provided by the gears mechanism between the base and the frame plaque, and 2-DOF (pitch and roll rotations) are provided by three actuators. The main object of this part is to study the 2-DOF

PMs without consideration of the yaw rotation ensured by the gears mechanism. Therefore, this study investigates the inverse kinematics of the 2-DOF parallel manipulators.

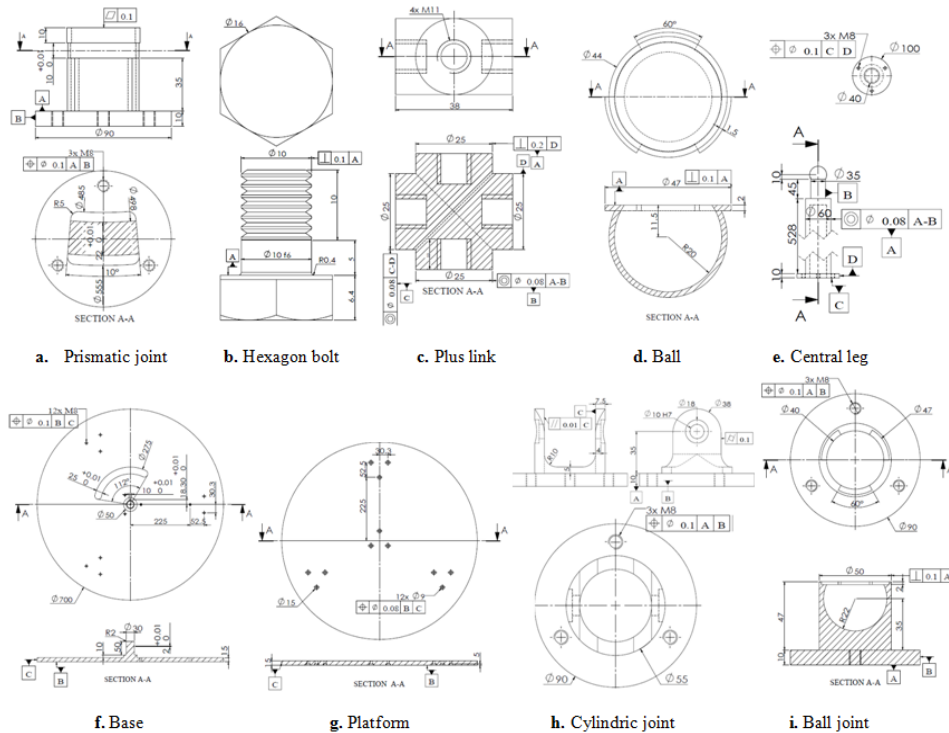


Fig. 5. Tolerance analysis of the parallel manipulators.

The choice of joints within the linear actuator itself is subjected to the overall movement of the platform which has to be two dimensional, i.e. with two degrees of freedom. Thus the upper and lower joints connecting the actuator to the base are universal (two rotational degrees of freedom). With the middle spherical joint (ball) connecting together the platform and the central leg which is forecasted to the base. With this configuration, the platform can only perform two needed pitch and roll rotations relatively to the base.

The 3UPU+1S (where U, P, and S denote universal, prismatic and spherical joint, respectively) PMs is composed of three UPU-type active actuators (legs) l_i ($i=1, 2, 3$) with the linear actuators, and one S-type active constrained leg l_0 with a linear actuator, a moving platform m and a fixed base B (Fig. 6.a), where the upper end-effectors form an equilateral ternary link $\Delta a_1 a_2 a_3$ with 3 sides $l_{mi} = l$, 3 vertices a_i ($i=1, 2, 3$) and a center point o . The lower end-effectors form an equilateral ternary link $\Delta A_1 A_2 A_3$ with 3 sides $L_i = L$, such as $L = l$, 3 vertices A_i ($i=1, 2, 3$) and a center point O .

Let $\{B\}$ be a coordinate system $O - XYZ$ fixed on B at O , $\{m\}$ be a coordinate system $o - xyz$ fixed on m at o . Each of l_i connects m to B by a universal joint U at a_i , an active leg l_i with a prismatic joint p_i ($i=1, 2, 3$) and a universal joint U at A_i . The S-type constrained leg l_0 connects m to B by a spherical joint S attached to m at o , and another end of l_0 perpendicularly fixed on B at O . The central leg l_0 limits three translation degrees of freedom of the moving

platform. The PMs platform has two rotations about X-axis and Y-axis respectively. In order to illustrate the rotation kinematic performance of the moving platform, the 3UPU+1S topological PMs with a general orientation is constructed in Fig. 6.b.

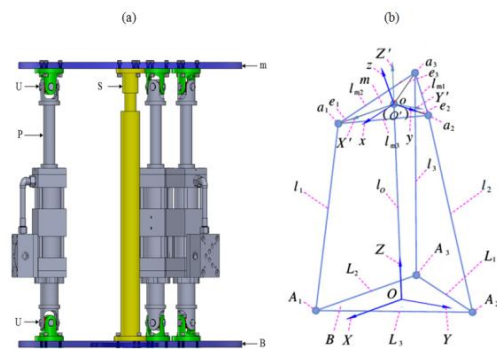


Fig. 6. The 3UPU+1S parallel manipulators.

When the mini-vehicle is moving over rough terrain, the chassis chain has a tendency to meet the shape of the ground. The result of this movement consists of two rotations pitch and roll of the chassis and parallel manipulators platform relatively to the horizontal plan. In this section we consider the two rotations pitch and roll of the PMs base as inputs of the inverse kinematics model. Then we try to bring the platform to the horizontal position by evaluating the extension and shortening, the velocity and acceleration corresponding of each of the three active actuators.

B. Inverse Position Kinematics

In roll-pitch-yaw formulation, all rotation matrix R^3 can be expressed as the product of three matrices as follows:

$$R_m^B = R_\psi \cdot R_\theta \cdot R_\varphi$$

$$R_m^B = \begin{pmatrix} \cos \psi & -\sin \psi & 0 \\ \sin \psi & \cos \psi & 0 \\ 0 & 0 & 1 \end{pmatrix} \cdot \begin{pmatrix} \cos \theta & 0 & \sin \theta \\ 0 & 1 & 0 \\ -\sin \theta & 0 & \cos \theta \end{pmatrix} \cdot \begin{pmatrix} 1 & 0 & 0 \\ 0 & \cos \varphi & -\sin \varphi \\ 0 & \sin \varphi & \cos \varphi \end{pmatrix}$$

The PMs considered can only perform pitch and roll rotations, therefore the yaw rotation equals to zero ($\psi = 0$). With this condition the orthogonal rotation matrix corresponding is:

$$R_m^B = \begin{pmatrix} \cos \theta & \sin \theta \sin \varphi & \sin \theta \cos \varphi \\ 0 & \cos \varphi & -\sin \varphi \\ -\sin \theta & \cos \theta \sin \varphi & \cos \theta \cos \varphi \end{pmatrix}$$

Let $\{A_i^B\}$ and $\{a_i^B\}$ be the coordinates of A_i and a_i in coordinate systems $O - XYZ$, respectively. And let $\{a_i^m\}$ be the coordinates of a_i in coordinate systems $o - xyz$. O^B is a vector of point o on m in $\{B\}$. They are expressed as follows:

$$A_i^B = \begin{pmatrix} X_{Ai} \\ Y_{Ai} \\ Z_{Ai} \end{pmatrix}, a_i^m = \begin{pmatrix} x_{ai} \\ y_{ai} \\ z_{ai} \end{pmatrix}, a_i^B = \begin{pmatrix} X_{ai} \\ Y_{ai} \\ Z_{ai} \end{pmatrix}, O^B = \begin{pmatrix} 0 \\ 0 \\ Z_0 \end{pmatrix}$$

$$R_m^B = \begin{pmatrix} u_x & v_x & w_x \\ u_y & v_y & w_y \\ u_z & v_z & w_z \end{pmatrix} \quad (1)$$

$$a_i^B = R_m^B \cdot a_i^m + O^B \quad (2)$$

where R_m^B is a rotation transformation matrix from $\{m\}$ to $\{B\}$. And $(u_x, u_y, u_z, v_x, v_y, v_z, w_x, w_y, w_z)$ which are nine orientation parameters of m in $\{B\}$, satisfy the following constraints:

$$\begin{aligned} u_x^2 + u_y^2 + u_z^2 &= v_x^2 + v_y^2 + v_z^2 = w_x^2 + w_y^2 + w_z^2 = 1 \\ u_x^2 + v_x^2 + w_x^2 &= u_y^2 + v_y^2 + w_y^2 = u_z^2 + v_z^2 + w_z^2 = 1 \\ u_x v_x + u_y v_y + u_z v_z &= u_x w_x + u_y w_y + u_z w_z = w_x v_x + w_y v_y + w_z v_z = 0 \end{aligned} \quad (3)$$

a_i^m and A_i^B ($i=1, 2, 3$) are derived as

$$\begin{aligned} a_1^m &= \frac{e}{2} \begin{pmatrix} \sqrt{3} \\ -1 \\ 0 \end{pmatrix}, a_2^m = \begin{pmatrix} 0 \\ -1 \\ 0 \end{pmatrix}, a_3^m = \frac{e}{2} \begin{pmatrix} -\sqrt{3} \\ -1 \\ 0 \end{pmatrix} \\ A_1^B &= \frac{e}{2} \begin{pmatrix} \sqrt{3} \\ -1 \\ 0 \end{pmatrix}, A_2^B = \begin{pmatrix} 0 \\ e \\ 0 \end{pmatrix}, A_3^B = \frac{e}{2} \begin{pmatrix} \sqrt{3} \\ -1 \\ 0 \end{pmatrix} \end{aligned} \quad (4)$$

where e is the same distance from a_i to O , and from A_i to O . From (2) and (4), a_i^B ($i=1, 2, 3$) are derived as:

$$\begin{aligned} a_1^B &= \frac{1}{2} \begin{pmatrix} \sqrt{3} e u_x - e v_x \\ \sqrt{3} e u_y - e v_y \\ \sqrt{3} e u_z - e v_z + 2Z_0 \end{pmatrix} = \frac{e}{2} \begin{pmatrix} \sqrt{3} \cos \theta - \sin \theta \sin \varphi \\ -\cos \varphi \\ -\sqrt{3} \sin \theta - \cos \theta \sin \varphi + \frac{2}{e} Z_0 \end{pmatrix} \\ a_2^B &= \begin{pmatrix} e v_x \\ e v_y \\ e v_z + Z_0 \end{pmatrix} = e \begin{pmatrix} \sin \theta \sin \varphi \\ \cos \varphi \\ \cos \theta \sin \varphi + \frac{1}{e} Z_0 \end{pmatrix} \\ a_3^B &= \frac{1}{2} \begin{pmatrix} -\sqrt{3} e u_x - e v_x \\ -\sqrt{3} e u_y - e v_y \\ -\sqrt{3} e u_z - e v_z + 2Z_0 \end{pmatrix} = \frac{e}{2} \begin{pmatrix} -\sqrt{3} \cos \theta - \sin \theta \sin \varphi \\ -\cos \varphi \\ \sqrt{3} \sin \theta - \cos \theta \sin \varphi + \frac{2}{e} Z_0 \end{pmatrix} \end{aligned} \quad (5)$$

Each of l_i ($i=1, 2, 3$) can be solved as

$$l_i^2 = |a_i^B - A_i^B|^2 = [(X_{Ai} - x_{ai})^2 + (Y_{Ai} - y_{ai})^2 + (Z_{Ai} - z_{ai})^2] \quad (6)$$

From (4) and (6), the formulae for solving l_i ($i=1, 2, 3$) are described as follows:

$$l_1^2 = \left[2e^2 + Z_0^2 + e^2 \left(\frac{\sqrt{3}}{2} \sin \theta \sin \varphi - \frac{3}{2} \cos \theta - \frac{1}{2} \cos \varphi \right) + Z_0 e (-\sqrt{3} \sin \theta - \cos \theta \sin \varphi) \right] \quad (7)$$

$$l_2^2 = [2e^2 + Z_0^2 - 2e^2 \cos \varphi + 2Z_0 e \cos \theta \sin \varphi] \quad (8)$$

$$l_3^2 = \left[2e^2 + Z_0^2 - e^2 \left(\frac{\sqrt{3}}{2} \sin \theta \sin \varphi + \frac{3}{2} \cos \theta + \frac{1}{2} \cos \varphi \right) + Z_0 e (\sqrt{3} \sin \theta - \cos \theta \sin \varphi) \right] \quad (9)$$

Therefore when given the orientation parameters (θ, φ) the lengths of the three active actuators l_i ($i=1, 2, 3$) of the moving PMs are solved.

C. Inverse Velocity Kinematics

Let δ_i be the unit vector of l_i and e_i the vector of the line oa_i ($i=1, 2, 3$) which can be solved as $\delta_i = \frac{1}{l_i} \begin{pmatrix} X_{ai} - X_{Bi} \\ Y_{ai} - Y_{Bi} \\ Z_{ai} - Z_{Bi} \end{pmatrix}$

$$\begin{aligned} \delta_1 &= \frac{1}{2r_1} \begin{pmatrix} \sqrt{3} e u_x - e v_x - \sqrt{3} e \\ \sqrt{3} e u_y - e v_y + e \\ \sqrt{3} e u_z - e v_z + 2Z_0 \end{pmatrix} = \frac{1}{2r_1} \begin{pmatrix} \sqrt{3} e \cos \theta - e \sin \theta \sin \varphi - \sqrt{3} e \\ e - e \cos \varphi \\ -\sqrt{3} e \sin \theta - e \cos \theta \sin \varphi + 2Z_0 \end{pmatrix} \\ \delta_2 &= \frac{1}{2r_2} \begin{pmatrix} e v_x \\ e v_y - e \\ e v_z + Z_0 \end{pmatrix} = \frac{1}{2r_2} \begin{pmatrix} e \sin \theta \sin \varphi \\ -e + e \cos \varphi \\ e \cos \theta \sin \varphi + Z_0 \end{pmatrix} \\ \delta_3 &= \frac{1}{2r_3} \begin{pmatrix} -\sqrt{3} e u_x - e v_x + \sqrt{3} e \\ -\sqrt{3} e u_y - e v_y + e \\ -\sqrt{3} e u_z - e v_z + 2Z_0 \end{pmatrix} = \frac{1}{2r_3} \begin{pmatrix} -\sqrt{3} \cos \theta - e \sin \theta \sin \varphi + \sqrt{3} e \\ e - e \cos \varphi \\ \sqrt{3} e \sin \theta - e \cos \theta \sin \varphi + 2Z_0 \end{pmatrix} \end{aligned} \quad (10)$$

Such as $r_i = [(X_{Ai} - x_{ai})^2 + (Y_{Ai} - y_{ai})^2 + (Z_{Ai} - z_{ai})^2]^{1/2}$

$$\begin{aligned} e_1 &= \frac{1}{2} \begin{pmatrix} \sqrt{3} e u_x - e v_x \\ \sqrt{3} e u_y - e v_y \\ \sqrt{3} e u_z - e v_z \end{pmatrix} = \frac{e}{2} \begin{pmatrix} \sqrt{3} \cos \theta - \sin \theta \sin \varphi \\ -\cos \varphi \\ -\sqrt{3} \sin \theta - \cos \theta \sin \varphi \end{pmatrix} \\ e_2 &= \begin{pmatrix} e v_x \\ e v_y \\ e v_z \end{pmatrix} = e \begin{pmatrix} \sin \theta \sin \varphi \\ \cos \varphi \\ \cos \theta \sin \varphi \end{pmatrix} \\ e_3 &= \frac{1}{2} \begin{pmatrix} -\sqrt{3} e u_x - e v_x \\ -\sqrt{3} e u_y - e v_y \\ -\sqrt{3} e u_z - e v_z \end{pmatrix} = \frac{e}{2} \begin{pmatrix} -\sqrt{3} \cos \theta - \sin \theta \sin \varphi \\ -\cos \varphi \\ \sqrt{3} \sin \theta - \cos \theta \sin \varphi \end{pmatrix} \end{aligned} \quad (11)$$

Let w be the rotational velocity of m expressed in $\{B\}$. The rotation motion can be divided into three rotations by (ψ, θ, φ) about three axes (X, Y, Z) with $(\psi = 0)$.

$$w = w_{(O,X,Y,Z)} = R_m^B \cdot w_{(o,x,y,z)} = \theta \cdot \begin{pmatrix} \sin \theta \sin \varphi \\ \cos \varphi \\ \cos \theta \sin \varphi \end{pmatrix} + \varphi \cdot \begin{pmatrix} \cos \theta \\ 0 \\ -\sin \theta \end{pmatrix} \quad (12)$$

Let V_0 and v_i be the velocity of the moving platform and point a_i , respectively $V_0 = (v_0 \ w)_{6 \times 1}^T$, $v_0 = 0$. No translation

velocity of m at point o .

$$w = (w_x, w_y, w_z)^T, v_i = w \times e_i \quad (13)$$

Let v_{li} ($i=1, 2, 3$) be the velocities along the active actuators l_i . Multiplication of δ_i with (13) gives us:

$$v_{li} = v_i \times \delta_i = (w \times e_i) \cdot \delta_i = (e_i \times \delta_i) \cdot w \quad (14)$$

$$\begin{pmatrix} v_{l1} \\ v_{l2} \\ v_{l3} \end{pmatrix} = \begin{pmatrix} (e_1 \times \delta_1)^T \\ (e_2 \times \delta_2)^T \\ (e_3 \times \delta_3)^T \end{pmatrix} \cdot \begin{pmatrix} w_x \\ w_y \\ w_z \end{pmatrix}$$

D. Inverse Acceleration Kinematics

Let a_{li} ($i=1, 2, 3$) be the accelerations along active actuators l_i , and ε the rotational acceleration of m , respectively. The time differentiation of (14) gives us:

$$a_{li} = \frac{d}{dt}((e_i \times \delta_i) \cdot w) = \left(\frac{d}{dt}(e_i \times \delta_i)\right) \cdot w + (e_i \times \delta_i) \cdot \left(\frac{d}{dt}w\right)$$

The resulting expression of the acceleration is given by:

$$a_{li} = ((w \times e_i) \times \delta_i + \frac{1}{l_i}(e_i \times (w \times e_i))) \cdot w + (e_i \times \delta_i) \cdot \varepsilon \quad (15)$$

VII. APPLICATION OF THE INVERSE KINEMATICS MODEL

The process for testing the inverse kinematics performance of the developed 3D-CAD model of the PMs includes input data and assuming a trajectory (terrain conditions) on which the mini-vehicle moves for a determined period of time. The range of rotations angles pitch and roll allowed by the PMS base and platform are $\theta \in [-30^\circ, 30^\circ]$, $\varphi \in [-30^\circ, 30^\circ]$. The input data are: the initial actuator's length $l_0 = 553$ mm, the coordinate $Z_0 = 553$ mm, and the distance $e = 260$ mm.

For testing the inverse kinematics model with the developed 3D-CAD model of the PMs we propose a trajectory on which the mini-vehicle moves during a period of time $t_i \in [t_0, t_{15}]$. Each time t_i represent a specific configuration of the terrain which can be depicted by a couple (θ, φ) of the rotation angles pitch and roll of the PMs Base. The rotational velocities and rotational accelerations of the PMs base and platform were selected by referring to the data used in inverse dynamics analysis for the 3UPS-UP parallel platform [10]. The input data used in this study is relatively large, therefore in this paper we only present a part of it. The input rotational angles, rotational velocities, and rotational accelerations are illustrated in Table II. Once the inverse kinematics model has been solved analytically, we pass to the code implementation. In this section we have used the software MATLAB to implement and execute the program solving the inverse kinematics of the PMs.

VIII. RESULTS AND DISCUSSION

The inverse kinematics problem was solved in MATLAB.

The results are shown in Table II and Fig. 7. a to Fig. 7. f.

The main object of the inverse kinematics analysis is how to act on the active actuators in order to maintain the PMS platform in the horizontal plane. Thus when the PMs base moves with a given orientation angles (θ, φ) , the platform is moved in the opposite sense with the same value of the orientation angles i.e. $(-\theta, -\varphi)$. For example, in Fig. 7.b at a given value of orientation angles $(\theta, \varphi) = (\frac{-\pi}{10}, \frac{-\pi}{10})$, the active actuators lengths, velocities and accelerations along these actuators are, respectively, ($l_1 = 445.875$ mm, $v_{l1} = -54.7114$ mm/s, $a_{l1} = 73.9978$ mm/s²), ($l_2 = 630.030$ mm, $v_{l2} = 41.0302$ mm/s, $a_{l2} = -44.1663$ mm/s²), ($l_3 = 584.410$ mm, $v_{l3} = 13.7325$ mm/s, $a_{l3} = -21.5616$ mm/s²), this means that to keep the PMs platform in the horizontal plane we must act on the three actuators by shortening the first actuator from its initial length 553 mm to 445.875 mm with a velocity of -54.7114 mm/s and an acceleration of 73.9978 mm/s², and by elongation of the second and the third actuators, respectively, from 553 mm to 630.030 mm with a velocity of 41.0302 mm/s and an acceleration of -44.1663 mm/s², and from 553 mm to 584.410 mm with a velocity of 13.7325 mm/s and an acceleration of -21.5616 mm/s².

The sign (-) of the velocity means that the actuator undergoes shortening. Since the PMs has three active actuators, to achieve the PMs platform stabilization the active actuators shortening and elongation are simultaneous and act in pair i.e. when two active actuators are respectively shortening or elongating the third one is elongating or shortening.

Furthermore, for specific configuration $(\theta, \varphi) = (0, 0), (\frac{\pi}{6}, \frac{\pi}{6}), (\frac{\pi}{8}, 0)$ which are shown in Fig. 7.a, Fig. 7.c, and Fig. 7.f, respectively, the PMs platform and the three active actuators movements are predictable. In the first configuration (0,0), the results indicate that the PMs platform still in stable position (horizontal plane) without any movement and the three active actuators keep their initial lengths (Fig. 7.a). When the orientation angles (θ, φ) are equal to $(\frac{\pi}{6}, \frac{\pi}{6})$ which are the two limit angles of the range of motion in our case (Fig. 7.c), the obtained results show that; while the first active actuator undergoes its highest elongation to attend 724.799 mm with its highest velocity of 102.748 mm/s, the two others undergo shortening such as ($l_2 = 446.548$ mm, $v_{l2} = -82.5111$ mm/s) and ($l_3 = 497.019$ mm, $v_{l3} = -19,6824$ mm/s). For the last specific configuration $(\theta, \varphi) = (\frac{\pi}{8}, 0)$ the rotation about X-axis (pitch rotation) is equal to zero, and then the only rotation of the PMs base is about the Y-axis (roll rotation) with $(\theta = \frac{\pi}{8})$ therefore the second active actuator which is in the plane XOZ does not undergo any shortening or elongation movement (Fig. 7.f), this is why its length still equal to the initial length $l_2 = 553$ mm and the velocity along this active actuator is equal to zero. As a result of this roll rotation, the first and the third active actuators move respectively by elongation and shortening movements to bring back the PMs Platform to the stabilized position.

TABLE II: ACTIVE ACTUATORS LENGTHS, VELOCITIES AND ACCELERATIONS ALONG THE THREE ACTIVE ACTUATORS FOR EACH COUPLE OF ORIENTATION ANGLES OF THE PMS BASE

t (s)	t ₀	t ₃	t ₅	t ₇	t ₁₁	t ₁₅
(θ, φ) (rad)	(0,0)	$(-\frac{\pi}{10}, -\frac{\pi}{10})$	$(\frac{\pi}{6}, \frac{\pi}{6})$	$(-\frac{\pi}{8}, \frac{\pi}{8})$	$(\frac{\pi}{10}, \frac{\pi}{14})$	$(\frac{\pi}{8}, 0)$
$(\dot{\theta}, \dot{\varphi}) \times 10^{-1}$ (rad/s)	(0,0)	(-1.6, -1.5)	(3.1, 2.8)	(-2.8, 2.5)	(0.9, 0.6)	(2.7, 0)
$(\ddot{\theta}, \ddot{\varphi}) \times 10^{-1}$ (rad/s ²)	(0,0)	(-2, -1.8)	(0.3, 0.2)	(-0.9, 0.9)	(1.1, 0.8)	(0.8, 0)
l_1 (mm)	553	445.875	724.799	512.893	650.406	639.397
l_2 (mm)	553	630.030	446.548	463.068	498.339	553
l_3 (mm)	553	584.410	497.019	686.155	510.946	467.147
v_{11} (mm/s)	0	-49.0424	85.4365	-26.3015	26.9035	56.7707
v_{12} (mm/s)	0	35.9500	-46.6948	-52.1473	-15.4459	0
v_{13} (mm/s)	0	14.8840	-26.6157	83.7646	-10.9588	-55.2758
a_{11} (mm/s ²)	0	73.9978	-20.3480	15.2776	-33.3975	-17.9646
a_{12} (mm/s ²)	0	-44.1663	38.4894	43.1329	21.5079	0
a_{13} (mm/s ²)	0	-21.5616	16.1266	-32.8357	13.5546	32.1473

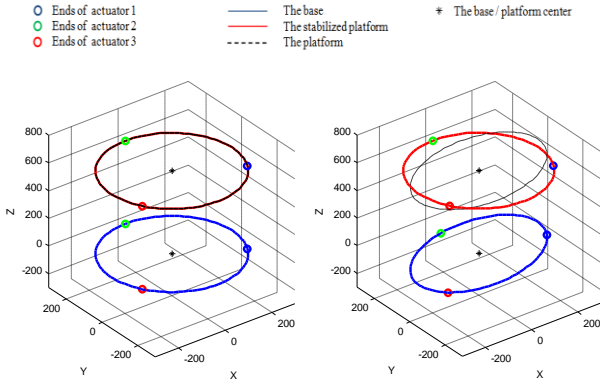


Fig. 7.a. (θ, φ) = (0,0)

Fig. 7.b. (θ, φ) = $(-\frac{\pi}{10}, -\frac{\pi}{10})$

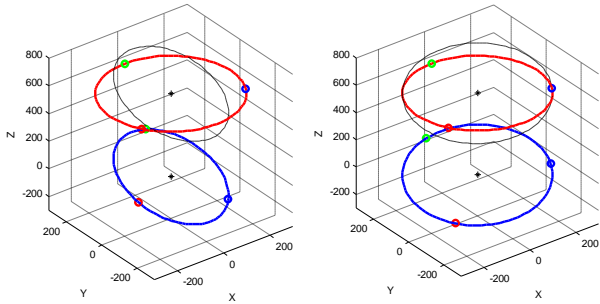


Fig. 7.c. (θ, φ) = $(\frac{\pi}{6}, \frac{\pi}{6})$

Fig. 7.d. (θ, φ) = $(-\frac{\pi}{8}, \frac{\pi}{8})$

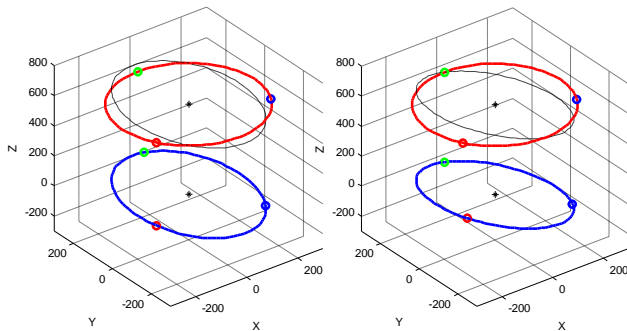


Fig. 7.e. (θ, φ) = $(\frac{\pi}{10}, \frac{\pi}{14})$

Fig. 7.f. (θ, φ) = $(\frac{\pi}{8}, 0)$

Fig. 7. Behavior of the PMS base and platform for each configuration of the PMS orientation angles during the mini-vehicle test period.

IX. CONCLUSION

The objective of this study is stated to design a tracked mini-vehicle with PMs as a mini-surface weapon platform which can fit some specific requirements regarding the desired movements. The main motivation of this work is to handle the varying disturbance characteristics from rough terrain and achieve the stabilization of the PMs platform during the tracked mini-vehicle movement on rough terrain.

In order to accomplish a suitable design of the mini-vehicle chassis and the PMs and make it realizable; a detailed tolerance analysis of each part composing the mini-vehicle, is done individually.

The trajectory adopted in the mini-vehicle test along the rough terrain combines both general and specific configurations of the PMs orientation to include all possible cases that could be encountered on real terrain.

The results of inverse kinematics model implementation under MATLAB show that the proposed inverse kinematics model is appropriate for the designed PMs and suitable for the stabilization task. The conformity and validity of inverse kinematics results can be attested through the specific configurations of the PMs base, which have provided predictable results. In fact the inverse kinematics implementation gives us the same results as expected in these particular configurations.

Application specific issues have not been taken into account. Therefore, the future tasks should include the following themes:

- 1) The realization of the parallel manipulators designed with respect to its shape and dimensions
- 2) The dynamics study of the 3-DOF parallel manipulators
- 3) Control of the designed 3-DOF parallel manipulators

ACKNOWLEDGMENT

Djoudi Farid would like to give much thanks to Qin Guojie and Xu Peng of Beijing Institute of Technology for their generous help in completing this work.

REFERENCES

- [1] G. Kumar, P. Y. Tiwari, V. Marcopoli, and M. V. Kothare, "A study of a gun-turret assembly in an armored tank using model predictive control," in *Proc. the 2009 conference on American Control Conference*, 2009, pp. 4848-4853.
- [2] D. Stewart, "A platform with six degrees of freedom," in *Proc. Institute of Mechanical Engineers*, vol. 180, no. 1, pp. 371-386, 1965.
- [3] V. E. Gough and S. G. Whitehall, "Universal tire testing machine," in *Proc. International Technical Congress FISITA, Institution of Mechanical Engineers*, UK, 1961, pp. 117.
- [4] K. M. Lee and D. K. Shah, "Kinematic analysis of a three degrees of freedom in-parallel actuated manipulator," in *Proc. IEEE Int'l conf. of Robotics and Automation*, 1987, pp. 345-350.
- [5] K. M. Lee and D. K. Shah, "Dynamic analysis of a three-degrees-of-freedom in-parallel actuated manipulator," *IEEE Trans. on Journal of Robotics and Automation*, vol. 4, no. 3, pp. 361-367, June 1988.
- [6] S. Alfayada, F. B. Oueddoua, F. Namounb, and G. Gheng, "High performance integrated electro-hydraulic actuator for robotics – part I: Principle, prototype design and first experiments," *Sensors and Actuators A: Physical*, vol. 169, pp. 115–123, 10 September 2011.
- [7] G. Cui and W. Hao, "Kinematic performance analysis on a new spatial rotation 3-dofs parallel robot mechanism," in *Proc. Third International Symposium on Intelligent Information Technology Application*, 2009, pp. 537-540.
- [8] D. C. H. Yang and T. W. Lee, "Feasibility study of a platform type of robotic manipulators from a kinematic viewpoint," *J. Mech. Transmiss. Automat. Des.*, vol. 106, pp. 191-198, June 1984.
- [9] E. F. Fichter, "A Stewart platform-based manipulator: general theory and practical construction," *Int. J. Robotics Res.*, vol. 5, no. 2, pp. 157-182, June 1986.
- [10] J. F. Li, W. H. Chen, D. Z. Liu, and J. S. Wani, "Inverse kinematic and dynamic analyses of a 3-dof parallel mechanism," in *Proc. Seventh International Conference on Control, Automation, Robotics And Vision (ICARCV'02)*, 2002, pp. 956-961.



Djoudi Farid was born in Tizi Ouzou-Algeria, on 10 September 1985. He was an engineer in mechanical design and manufacturing from MPS, Algiers, Algeria in June 2010. His scientific research includes biomechanics, the knee joint, especially in design and analysis of Total Knee Prosthesis (TKP) with a published article entitled: 3D reconstruction of bony elements of the knee joint and finite element analysis of total knee prosthesis obtained from the reconstructed model. Temporary, he is studying in School of Mechatronical Engineering, Beijing Institute of Technology; Beijing – China as a master of science candidate in the field of mechanical design and control.



Li Dongguang was born in Dandong City, Liaoning Province, China, on 7 June 1965. He got his PhD degree in precision instruments and optoelectronics engineering, Tianjin University, Tianjin, China; M.E. in precision instruments and optoelectronics engineering, Tianjin University; B.E. in precision instruments engineering, Tianjin University. He is now a professor, PhD supervisor, School of Mechatronical Engineering, Beijing Institute of Technology, the director of the Lab of Mechanotronics Dynamic Control, gets great achievements and has high academic influence. Have co-published one teaching materials, and more than twenty papers included by EI, five papers included by ISTP.